Heliyon 9 (2023) e22595

Contents lists available at ScienceDirect

Heliyon

journal homepage: www.cell.com/heliyon

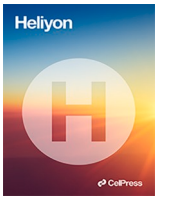

METTL3/YTHDC1-mediated upregulation of LINC00294 promotes hepatocellular carcinoma progression

Rulin Zhang [a,1], Rui Yang [a,b,c,1], Zhuodeng Huang [a,b,c,1], Xiang Xu [a,b,c], Siang Lv [a,b,c], Xin Guan [a], Hao Li [d,e,**], Jun Wu [a,b,c,*]

[a] *Department of Laboratory Medicine, Jiading Branch of Shanghai General Hospital, Shanghai Jiao Tong University School of Medicine, Shanghai 201803, China*
[b] *Department of Pathology, The Affiliated Hospital of Youjiang Medical University for Nationalities, Baise 533000, China*
[c] *The Key Laboratory of Molecular Pathology (Hepatobiliary Diseases) of Guangxi, Baise 533000, China*
[d] *Organ Transplantation Clinical Medical Center of Xiamen University, Department of Organ Transplantation, Xiang'an Hospital of Xiamen University, School of Medicine, Xiamen University, Xiamen, 361005, Fujian, China*
[e] *Department of Pancreatic Surgery, Shanghai Cancer Center, Fudan University, Shanghai, 200032, China*

ARTICLE INFO

Keywords:
LINC00294
N^6-methyladenosine modification
METTL3
YTHDC1
Hepatocellular carcinoma

ABSTRACT

Hepatocellular carcinoma (HCC) is a highly prevalent malignancy and the third highest contributor to cancer-associated deaths globally. Research has increasingly demonstrated a strong correlation between long noncoding RNAs (lncRNAs) and the incidence and progression of HCC. Nonetheless, the exact mechanism whereby the function of lncRNAs in HCC has not been elucidated. This study explored the pathological role of LINC00294 in HCC, as well as the modulatory mechanism involved. Based on the "The Cancer Genome Atlas (TCGA)" database and validation in HCC cell lines and tissues, the expression of LINC00294 was discovered to be upregulated in HCC tissues and correlated with tumor grade and the prognosis of patients with HCC. Functionally, LINC00294 stimulated the proliferation of HCC cells as well as the Warburg effect (aerobic glycolysis) to enhance progression of tumor *in vivo*. Mechanistically, METTL3/YTHDC1-mediated N^6-methyladenosine (m^6A) modification underwent a significant enrichment within LINC00294 and was shown to enhance its RNA stability. Moreover, LINC00294 promoted the interaction between YTHDC1 and HK2 and GLUT1 mRNA. Overall, our study illustrates the m^6A modification-mediated epigenetic mechanism of LINC00294 expression and regulatory role in HK2and GLUT1 mRNA expression and indicate LINC00294 as a potential biomarker panel for prognostic prediction and treatment in HCC.

1. Introduction

Hepatocellular carcinoma (HCC) is one of the most prevalent malignancies and is the third most common contributor to cancer-

* Corresponding author. Department of Laboratory Medicine, Jiading Branch of Shanghai General Hospital, Shanghai Jiao Tong University School of Medicine, Shanghai 201803, China.
** Corresponding author. Organ Transplantation Clinical Medical Center of Xiamen University, Department of Organ Transplantation, Xiang'an Hospital of Xiamen University, School of Medicine, Xiamen University, Xiamen, 361005, Fujian, China.
E-mail addresses: lihao6656@163.com (H. Li), jun.wu@shsmu.edu.cn (J. Wu).
[1] These authors contributed equally to this work.

https://doi.org/10.1016/j.heliyon.2023.e22595
Received 9 May 2023; Received in revised form 6 November 2023; Accepted 15 November 2023
Available online 23 November 2023

associated mortality worldwide [1]. Despite remarkable advancements in the medical management of HCC in recent years that include surgical intervention, transhepatic arterial chemotherapy and embolization, targeted therapy, liver transplantation, and immunotherapeutic treatment, the elevated metastatic rate and postsurgical recurrence rate still produce an unfavorable prognosis for patients with HCC [2,3]. Specifically, the complex genetic and epigenetic mechanisms regulating the incidence and progression of HCC are the cause of this phenomenon [2]. Consequently, understanding the fundamental processes involved in the incidence and progression of HCC etiology and identifying novel molecular targets and efficient diagnostic approaches are critical for treating patients with HCC.

Long non-coding RNA (lncRNA) are RNA molecules that comprise >200 nucleotides that lack or have limited coding ability [4,5]. Accumulating research shows that lncRNAs are important regulatory factors for multiple biological functions and perform a fundamental function in tumor proliferation, invasion, metastasis, and metabolic process [6–8]. LncRNA H19, LOC285194, TINCR, and HAND2-AS1 play key roles in the regulation of tumor proliferation, migration, and invasion [9–12]. Consequently, a deeper understanding of the lncRNA-associated gene-modulatory processes will support the development of viable prognostic biological markers and personalized therapies for patients with HCC. LINC00294, a newly described long intergenic non-protein coding RNA identified in recent years, has been reported to be related to atherosclerotic plaque and ischemic stroke and the activation of human retinal vascular endothelial cells [13,14]. Bakkenolide-IIIa-mediated upregulation of LINC00294 expression was shown to ameliorate LPS-induced inflammatory injury in human umbilical vein endothelial cells [15]. In tumors, the elevation of LINC00294 expression was reported to be related to the malignant phenotype of human cervical cancer [16]. Conversely, LINC00294 overexpression could inhibit the malignant progression of colorectal carcinoma and glioma [17,18], suggesting that LINC00294 plays distinct roles in different types of tumors. Nevertheless, the significance of LINC00294 in the progression of HCC remains largely unknown, and more research is urgently needed to clarify the role of LINC00294 in HCC. As the most prevalent RNA modification, N^6-methyladenosine (m^6A) plays a crucial role in multiple biological activities [19]. The m^6A gene is dynamically modulated to perform important functions in various biological processes [20]. The network of m^6A regulation can be altered by the combined functions of the "writer," which adds the m^6A modification; the "reader," which recognizes and binds the m6A modification to enable its roles; and the "eraser," which removes methylation activity [20]. Recently, the m6A modifications and related genes have become research hotspots as being involved in multiple tumorigenic processes. The methyltransferase activity of METTL3 affects several biological processes and plays multiple roles in cancers. Studies suggested that diverse signals and pathways in cancers are regulated by METTL3, including cell proliferation, invasion, metastasis, and drug resistance. The expression of METTL3 in breast cancer enhances the expression of HBXIP and contributes to positive feedback between HBXIP/let-7g/METTL3/HBXIP and cell proliferation [21]. In addition, METTL3 deficiency influences reprogramming in macrophages and can enhance tumor progression in mouse models thereby eliminating the efficacy of PD-1 blockade treatment [22].

The present study sought to elaborate the role of LINC00294 in HCC. We determined the pattern of LINC00294 expression in tissue samples and the correlation between this and the prognosis of patients with HCC. Furthermore, the effects of s overexpression and RNA interference on HCC proliferation and glycolytic metabolism were investigated. Mechanistically, the METTL3/YTHDC1-mediated LINC00294 m^6A epitranscriptomic change in tumorigenesis and glycolysis pathways was assessed during these processes. Thus, this study produced unique insights into potential therapeutic approaches for HCC.

2. Method and materials

2.1. Bioinformatics analysis

Gene expression information was gathered from The Cancer Genome Atlas (TCGA) for HCC and included 374 cases of tumor tissues and 50 cases of normal tissues. The GSEA algorithm was employed to analysis the LINC00294 expression in both nonpaired and paired HCC tissues in TCGA.

2.2. Tissue microarray

The relative expression of LINC00294 in HCC tissues were detected by in situ hybridization (ISH) with a specific digoxin-labeled LINC00294 probe (digoxin-5'-TACCATAGCCCAATATTGGTATTTCCGAGCATGGATGTTT-3′-digoxin) (Boster, Wuhan, China) on a tissue microarray (Outdo Biotech, Shanghai, China) containing 94 paraffin-embedded HCC samples. Briefly, the dewaxed and rehydrated tissues were hybridized with the specific LINC00294 probe at 4 °C overnight, then incubated with anti-digoxin-AP (Roche, Basel, Switzerland) at 4 °C overnight and stained with NBT/BCIP and quantified.

2.3. Animals

Approval for animal experiments conducted in this study was granted by the Shanghai General Hospital Clinical Center Laboratory Animal Welfare & Ethics Committee. Four-week-old nude mice (three per group, obtained from Shanghai Lab Animal Research Center, Shanghai China) were subcutaneously injected with 5×10^6 Huh7 cells. The tumor volume was assessed every three days for four weeks. The equation was as follows: volume = length × $width^2/2$.

2.4. Cell culture and generation of the stable cell line

Human normal hepatocyte THLE-2 cells and HCC cell lines (HepG2, PLC/PRF/5, MHCC97h, Huh7, and Hep3B were obtained from

the American Type Culture Collection (Manassas, VA, USA) supplied, which were cultured in RPMI 1640 medium or Dulbecco's modified Eagle medium (BI, Israel) supplemented with 10 % fetal bovine serum (FBS, BI, Israel), and streptomycin and penicillin (100 μg/mL each). Cells were incubated at a 37 °C in 5 % CO_2.

LINC00294 expression in HepG2 and Huh7 cells were knocked down with the aid of the lentiviral particles that expressed scrambled control or shRNA (RiboBio, Guangzhou, China) as previously described [23]. The LINC00294 and shRNAs were constructed, cloned into pLVX-puro (Clontech, Palo Alto, CA, USA). The lentivirus-expressing short hairpin RNA (shRNA) oligos targeting LINC00294 (sh-LINC00294), was produced in 293T cells along with packaging plasmids psPAX2 and pMD2.G and cultured for 48 h for supernatant collection. For stable shRNA overexpression, HCC cells transfected with the collected supernatant were selected with puromycin (MCE, USA) at 10 μg/mL for three weeks and then validated by qPCR. Supplementary Table 1 lists the sequences of shRNAs.

2.5. Hematoxylin-eosin staining

Hematoxylin-eosin (H&E) staining was performed to assess the pathological changes in the tumor tissue. Briefly, tumor tissues were fixed in 10 % neutral buffered formalin. The standard method of dehydration, clearing in xylene, and paraffin embedding were used. Sections of 5-μm thickness were cut by a rotary microtome. After deparaffinizing, the liver tissue sections were stained using H&E and Masson-trichrome staining kits. Finally, histopathological changes were observed with an optical microscope (Olympus, Japan).

2.6. TUNEL staining

Tissue sample sections were permeabilized for 20 min using 0.5 % Triton X-100 and rinsed three more times with phosphate-buffered saline. Samples were then stained for 20 min using nonimmune animal serum and then by overnight staining with the TUNEL assay kit (Beyotime, Shanghai, China) at 37 °C in the dark. After washing, DAPI was used to stain nuclei for 5 min in the dark, followed by PBST (PBS with 0.5 % Triton X-100) rinsing and imaging via fluorescence microscopy (Olympus, Japan).

2.7. Cell viability assay

The viability of HCC cells was determined with a cell counting kit-8 (CCK-8) assay and via colony formation. A total of 2.0×10^3 cells were seeded into a 96-well plate. Subsequently, 10 μL of CCK-8 reagent was added into each well at different time points and then incubated for 2 h. The optical density was measured with a utilizing Multiskan™ FC System (Thermo Scientific) at 450 nm. For colony formation analysis, 500 HCC cells were seeded into 6-well culture plates for the colony formation assay. Cells were incubated for 10 days and then fixed using 4 % paraformaldehyde before staining with 0.1 % crystal violet. Subsequently, cells were rinsed in water and dried. The colonies were then counted.

2.8. Apoptosis assay

To investigate the mechanism whereby apoptosis occurred following drug administration or cell transfection, we employed the Annexin V-FITC/propidium iodide (PI) Apoptosis Detection Kit (Beyotime, Haimen, China) according to the manufacturer instructions. A total of 5×10^5 cells/mL were mixed with 500 μL of binding buffer with 5 μL of PI and 5 μL of Annexin V-FITC. Flow cytometry (NovoCyte, ACEA Biosciences, San Diego, CA, USA) was performed to determine if cells had undergone apoptosis following 15 min of incubation. FlowJo was used for data analyses.

2.9. Lactate synthesis, glucose absorption, and extracellular acidification rate

To assess the glycolysis in HCC cells, analysis of lactate synthesis, glucose absorption, and extracellular acidification rate (ECAR) analysis was performed. The Lactate Assay kit (Bio Vision, Mountain View, CA, USA) was used to quantify the lactate concentration, while the glucose assay kit (Sigma, St-Louis, MO, USA) was used to quantify the level of glucose uptake. The ECAR was analyzed using the Seahorse XF 96 Extracellular Flux Analyzer (Agilent Technologies, Santa Clara, CA, USA). HCC cells were incubated in 96-well plates overnight, and after measurement of baseline concentration, glucose, oligomycin, and 2-DG were sequentially added into each well for ECAR measurement.

2.10. RNA stability assay

Actinomycin D (2 μg/mL), an RNA synthesis antagonist, was used to treat cells, and the RNA stability was assessed at 12 h after treatment. RNA was isolated at various time intervals in accordance with the manufacturer's recommendations for extraction. Briefly, total RNA was extracted from cells with the aid of Trizol reagent (Invitrogen) and subsequently synthesized into cDNA using PrimeScript™ 1st Strand cDNA Synthesis Kit (Takara). The qRT-PCR on ABI StepOne Plus System (Takara) based on a standard procedure from the SYBR® Green Premix Pro Taq HS qPCR Kit (Takara) was performed using the corresponding primer pairs (Supplementary Table 2).

2.11. RNA fluorescent in situ hybridization

The cellular location of LINC00294 was assessed with a fluorescent in situ hybridization (FISH) kit (RiboBio, China). Each lncRNA sequence was targeted by multiple probes to provide an adequate signal-to-background ratio. The appropriate signal intensity was delivered by a collection of 15–20 probes that spanned the whole length of the RNA molecule, with each probe containing multiple fluorophores. Resuspension of the pooled FISH probes was performed in an RNase-free storage buffer at a final concentration of 25 μM and kept at −20 °C in the dark. FISH was imaged with the aid of a confocal device (Leica TCS-SP8).

2.12. Luciferase reporter assay

The regulatory relationship between METTL3 and LINC00294 was detected with a luciferase reporter assay. The LINC00294 full-length transcript was cloned into the pmirGLO plasmid (Promega). Furthermore, the adenosine bases within the m6A consensus sequences were substituted with cytosine to constructed the mutant LINC00294 reporter plasmid. Cells were then transfected with the LINC00294 reporter plasmid, both in its wild-type and mutant forms. After 48 h, the Dual-Luciferase™ Reporter (DLR™) Assay System was used to measure luciferase activity, which was based on the relative ratio of firefly luciferase activity to the luciferase activity of renilla.

2.13. Methylated RNA immunoprecipitation-qPCR assay

Methylated RNA immunoprecipitation (MeRIP)-qPCR was used to test the relative levels of m^6A in LINC00294 in HCC cells with knockdown of METTL3. Briefly, purified mRNA from HCC cells was digested with DNase I and then fragmented into small fragments using RNA fragmentation reagent and incubated at 94 °C. Thereafter, the stop buffer was added, and the fragments were precipitated. The anti-m6A antibody (12 μg) was preincubated with 50 μL beads in immunoprecipitation buffer for 1 h at 25 °C. Then, 6 μg of fragment RNA was added to the antibody-beads mixture and incubated for 4 h at 4 °C on a rotator. After adequate washing, the immunoprecipitated mixture was digested using high concentration of proteinase K, and the bound RNA was extracted and used for qPCR analysis. The $2^{-\Delta\Delta Ct}$ technique was used to assess the relative enrichment in comparison with the input group.

2.14. RNA immunoprecipitation

RNA immunoprecipitation (RIP)-qPCR was used to analyze the enrichment of METTL3 on LINC00294 in HCC cells. The Magna RIP Kit (17–700, Millipore, MA) was used to perform the RIP assay. First, 5 μg of anti-METTL3 (Abcam, USA), anti-YTHDC1 (Abcam, USA), and anti-rabbit IgG (Millipore, Germany) were incubated with 50 μL of magnetic beads before cell lysates were added. Then, the RNA-protein IP complexes were washed six times and proteinase K digestion buffer was added to remove proteins. Finally, RNA was extracted via phenol-chloroform RNA extraction and purified for qPCR analysis. Normalization of the relative enrichment was performed using $\%Input = 1/10 \times 2^{Ct\ [IP]-Ct\ [input]}$. done to the input as: $\%Input = 1/10 \times 2^{Ct\ [IP]\ -\ Ct\ [input]}$.

2.15. RNA extraction, nuclear-cytoplasmic fractionation, and quantitative RT-qPCR

RT PCR was performed to test relative mRNA/RNA expression levels in HCC cells or tissues. Total RNA was extracted from cells or tissues with Trizol reagent (Invitrogen). Nuclear and Cytoplasmic Extraction Reagents (ThermoFisher, CA, USA) were used to extract nuclear fractionation and cytoplasmic RNA following the manufacturer's protocol. RNA subsequently synthesized into cDNA using PrimeScript™ 1st Strand cDNA Synthesis Kit (Takara). RT-qPCR was conducted on an ABI StepOne Plus System (Takara) using the corresponding primer pairs (Supplementary Table 2). The mRNA expression levels in cells were normalized to those of GAPDH or U6.

2.16. Western blot

The relative protein level in HCC cells was determined via western blotting. Briefly, total protein was extracted from HCC cells using pre-chilled RIPA buffer (Beyotime, Shanghai, China). After protein quantification, equal amounts of protein were loaded onto 10 % SDS-PAGE for electrophoresis. Separated proteins were then blotted onto 0.45 μm polyvinylidene fluoride membranes (Millipore, USA). Membranes were then blocked with 5 % non-fat milk in TBST for 1.5 h and then incubated with primary antibodies at 4 °C overnight (Supplementary Table 3). Blots were then washed three times with TBST and incubated with corresponding secondary antibodies at room temperature for 1 h. Detection of immunoblots was performed using an imaging system (Bio-Rad, USA).

2.17. Statistical analysis

SPSS software (version: 22.0, Chicago, USA) was used for all data analyses. The Student's *t*-test was used to compare the differences between two groups. One-way ANOVA was used for comparing the differences between multiple groups, followed by Tukey's multiple comparisons test. Paired *t*-test was used to compare the expression level of lncRNA- LINC00294 in primary HCC tissues and normal adjacent tissues. Group $\chi 2$ test was adopted to analyze the associations of the expression of LINC00294 in HCC tissues with the clinicopathological features of patients. Receiver Operating Characteristic (ROC) analyses were performed to detect the diagnostic value of LINC00294 in HCC. Cox proportional hazard regression model was, respectively, chosen for single factor analysis and multiple

factor analysis of survival. The survival curves of patients with HCC were plotted using the Kaplan–Meier technique and the log-rank test. A *P*-value <0.05 was considered significant.

3. Results

3.1. Relationship between LINC00294 and the clinical characteristics of patients with HCC

To identify the pattern of LINC00294 expression, we assessed the expression of LINC00294 in HCC from TCGA database and observed the upregulation of LINC00294 expression in 374 HCC tissues compared to 50 normal liver tissues (Fig. 1A). Meanwhile, the

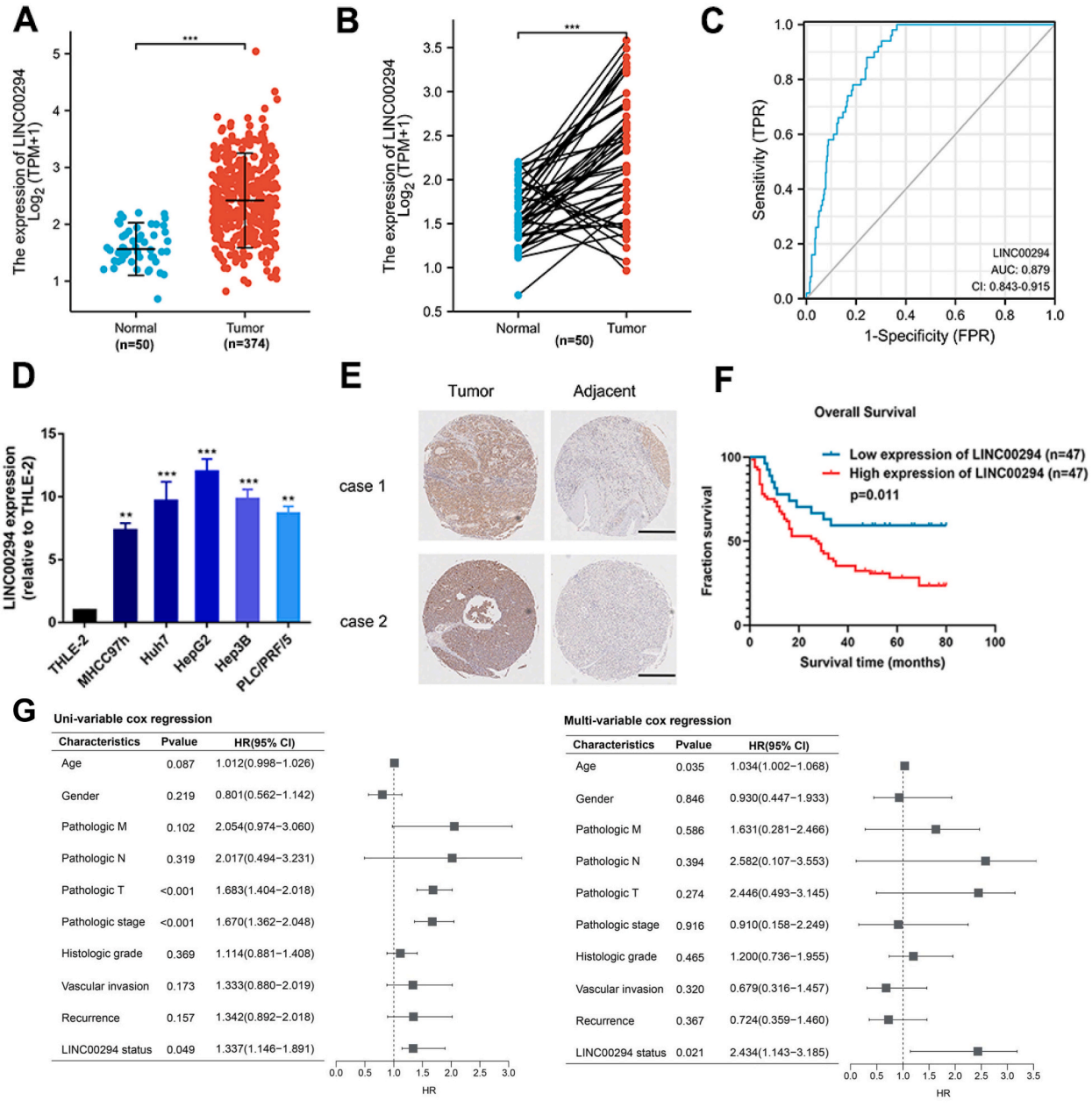

Characteristics	Pvalue	HR(95% CI)
Age	0.087	1.012(0.998–1.026)
Gender	0.219	0.801(0.562–1.142)
Pathologic M	0.102	2.054(0.974–3.060)
Pathologic N	0.319	2.017(0.494–3.231)
Pathologic T	<0.001	1.683(1.404–2.018)
Pathologic stage	<0.001	1.670(1.362–2.048)
Histologic grade	0.369	1.114(0.881–1.408)
Vascular invasion	0.173	1.333(0.880–2.019)
Recurrence	0.157	1.342(0.892–2.018)
LINC00294 status	0.049	1.337(1.146–1.891)

Characteristics	Pvalue	HR(95% CI)
Age	0.035	1.034(1.002–1.068)
Gender	0.846	0.930(0.447–1.933)
Pathologic M	0.586	1.631(0.281–2.466)
Pathologic N	0.394	2.582(0.107–3.553)
Pathologic T	0.274	2.446(0.493–3.145)
Pathologic stage	0.916	0.910(0.158–2.249)
Histologic grade	0.465	1.200(0.736–1.955)
Vascular invasion	0.320	0.679(0.316–1.457)
Recurrence	0.367	0.724(0.359–1.460)
LINC00294 status	0.021	2.434(1.143–3.185)

Fig. 1. Overexpression of LINC00294 indicates poor prognosis in patients with HCC. (A–B) LINC00294 expression in both non-paired and paired HCC tissues in TCGA database. **(C)** ROC curve of LINC00294 expression. **(D)** The expression level of LINC00294 between HCC cell lines and THLE-2 cells were assessed by RT-qPCR. **(E)** Representative images of LINC00294 expression in HCC tissues were detected by ISH assays, scale bar, 500 μm. **(F)** Kaplan-Meier curves for overall survival in HCC for all cases. **(G)** Univariate and multivariate analysis of overall survival in HCC patients. *p < 0.05; **p < 0.01; ***p < 0.001.

expression of LINC00294 was found to be higher in HCC samples than that in paired normal liver samples (Fig. 1B). Moreover, it demonstrated that the expression of LINC00294 was correlated with the age, pathological grade, and tumor recurrence, but no significant difference could be found regarding the gender, pathologic M, N, T, and pathologic stage of patients between LINC00294 low and high expression group (Table 1). Evaluation of the diagnostic value of LINC00294 via the ROC analysis showed that the Area Under the Curve (AUC) of LINC00294 was 0.879 (Fig. 1C). Furthermore, the expression of LINC00294 was measured in different HCC cell lines (MHCC97h, Huh7, HepG2, Hep3B, and PLC/PRF/5) and human normal hepatocyte THLE-2 cells. LINC00294 expression was markedly upregulated in the HCC cell lines in contrast with that in THLE-2 cells (Fig. 1D). The ISH analysis showed that the LINC00294 expression was higher in cancer tissues than that in paired normal adjacent tissues in the tissue microarray (Fig. 1E). Furthermore, the survival analysis showed a negative correlation between the elevated LINC00294 expression level and the overall survival of patients with HCC (Fig. 1F). In terms of overall survival, univariate along with multivariate analysis revealed that LINC00294 expression was an independent prognostic factor (Fig. 1G).

3.2. *LINC00294 promotes HCC proliferation and inhibit apoptosis*

To examine the biological activity of LINC00294 in HCC cells, we constructed stable knockdown and overexpression of LINC00294 in HepG2 and Huh7 cells, which were measured by RT-qPCR (Supplementary Figs. 1A and B). We then conducted the CCK-8 and colony formation assays, and findings demonstrated that knockdown of LINC00294 decreased the proliferation rate and inhibited the colony-forming ability, whereas the overexpression of LINC00294 promoted cell proliferation and clonal formation (Fig. 2A and B). We then performed flow cytometry with the Annexin V/PI double staining assay to analyze the number of apoptotic cells after downregulating of LINC00294 expression. As opposed to that in the control group, LINC00294 knockdown in HepG2 and Huh7 cells had a higher apoptotic rate (Fig. 2C). Moreover, to identify the promotion of LINC00294 in HCC proliferation *in vivo*, Huh7 cells with LINC00294 knockdown or overexpression and control cells were administered to nude mice via subcutaneous injection for tumor xenograft. Subsequently, we found that the silencing of LINC00294 suppressed tumor growth and that the tumors in the sh-LINC00294 group exhibited lesser weights and smaller sizes as opposed to those in the control group (Fig. 2D–F). The HE staining and TUNEL assay showed the apoptotic rate of tumor cells was reduced by LINC00294 overexpression and enhanced in the sh-LINC00294 group (Fig. 2G).

Table 1
LINC00294 expression and clinical features of patients with HCC.

characteristics total cases	N of case 373[a]	LINC00294		*P* value
		Low(N = 186)[a]	High(N = 187)[a]	
Age(years)				
≤60	177	72	105	0.0009
>60	195	113	82	
Gender				
Male	252	129	123	0.5073
Female	121	57	64	
Pathologic_M				
M0	267	126	141	0.3498
M1	4	3	1	
Pathologic_N				
N0	253	119	134	0.1262
N1	4	0	4	
Pathologic_T				
T1	182	97	85	0.3273
T2	95	47	48	
T3	80	36	44	
T4	13	4	9	
Pathologic_stage				
I	172	90	82	0.2514
II	87	45	42	
III	85	34	51	
IV	5	3	2	
Neoplasm histologic grade				
G1	55	36	19	0.0033
G2	178	96	82	
G3	123	48	75	
G4	12	4	8	
Vascular invasion				
Yes	110	54	56	0.5552
No	207	110	97	
Tumor recurrence				
Yes	141	60	81	0.0329
No	179	98	81	

[a] The reason for the inconsistent number of cases is incomplete collection of patient information from TCGA database.

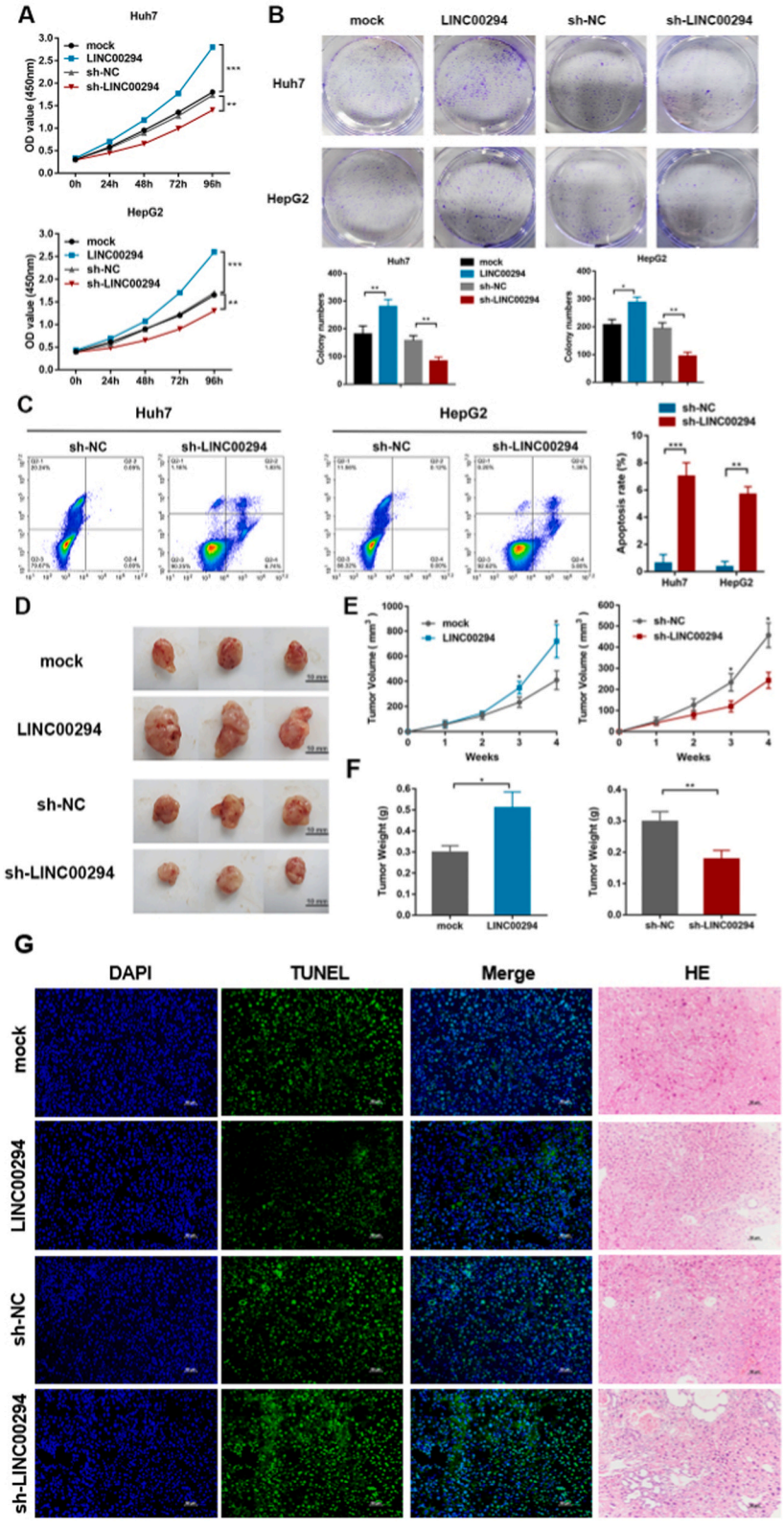

(caption on next page)

Fig. 2. LINC00294 promotes HCC proliferation *in vitro* and *in vivo*. (A) The CCK8 assay was performed in Huh7 and HepG2 cells with LINC00294 over-expression and knockdown. **(B)** The colony formation assay was performed in Huh7 and HepG2 cells. **(C)** The apoptosis rate in control and LINC00294 knockdown cells. **(D)** Representative images of subcutaneous tumors in nude mice, scale bar, 1 cm. **(E–F)** The tumor growth volume and weight measurements of nude mice. **(G)** The TUNEL and H&E staining of HCC tumor tissues. *p < 0.05, **p < 0.01, ***p < 0.001.

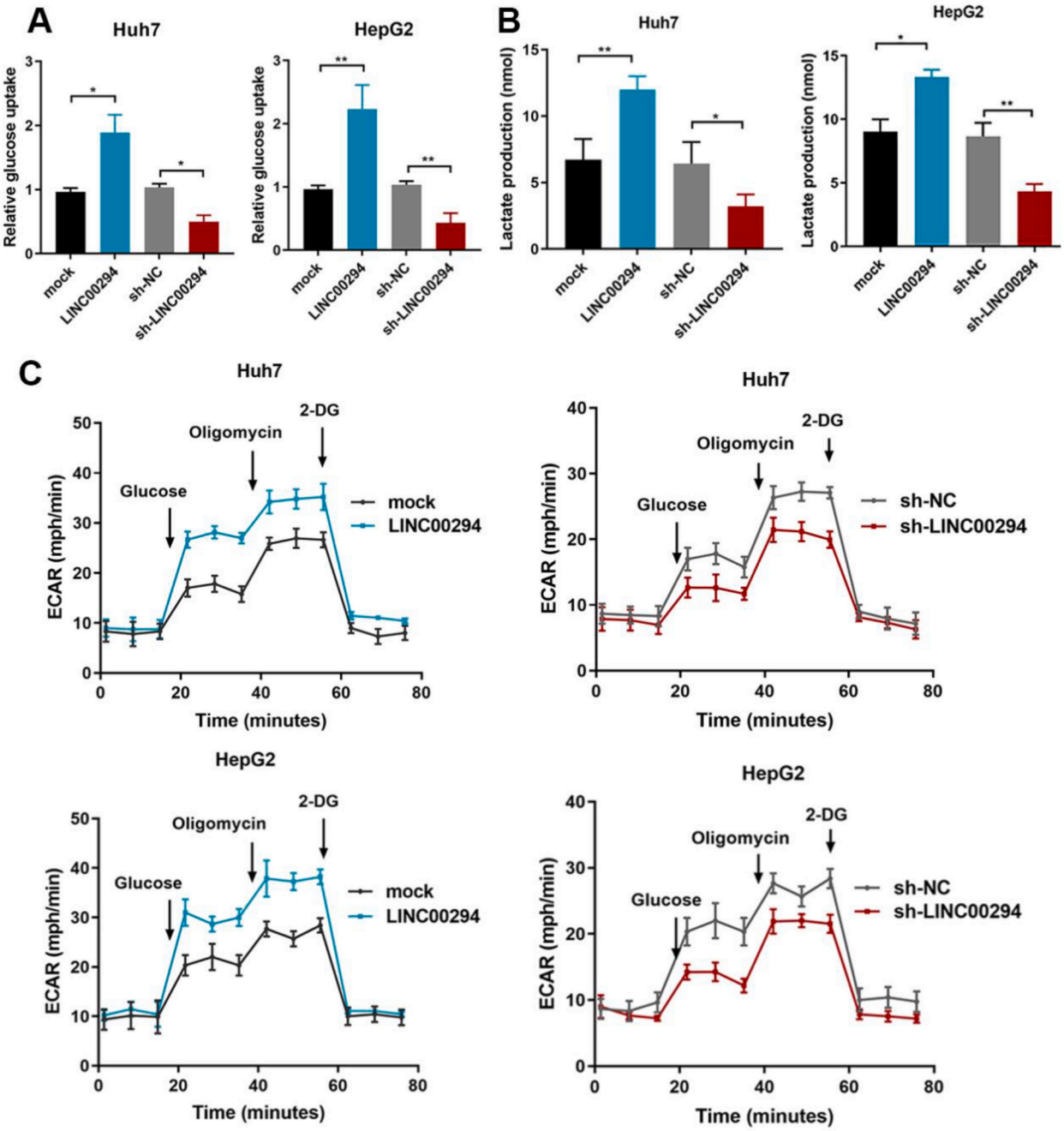

Fig. 3. LINC00294 drives glycolytic metabolism in HCC. (A) Glucose uptake were measured by colorimetric analysis with Huh7 and HepG2 cells with LINC00294 over-expression and knockdown. **(B)** Lactate production was measured in HCC cells by colorimetric analysis. **(C)** ECAR profiles were detected for the glycolytic capacity of LINC00294 overexpression and knockdown.

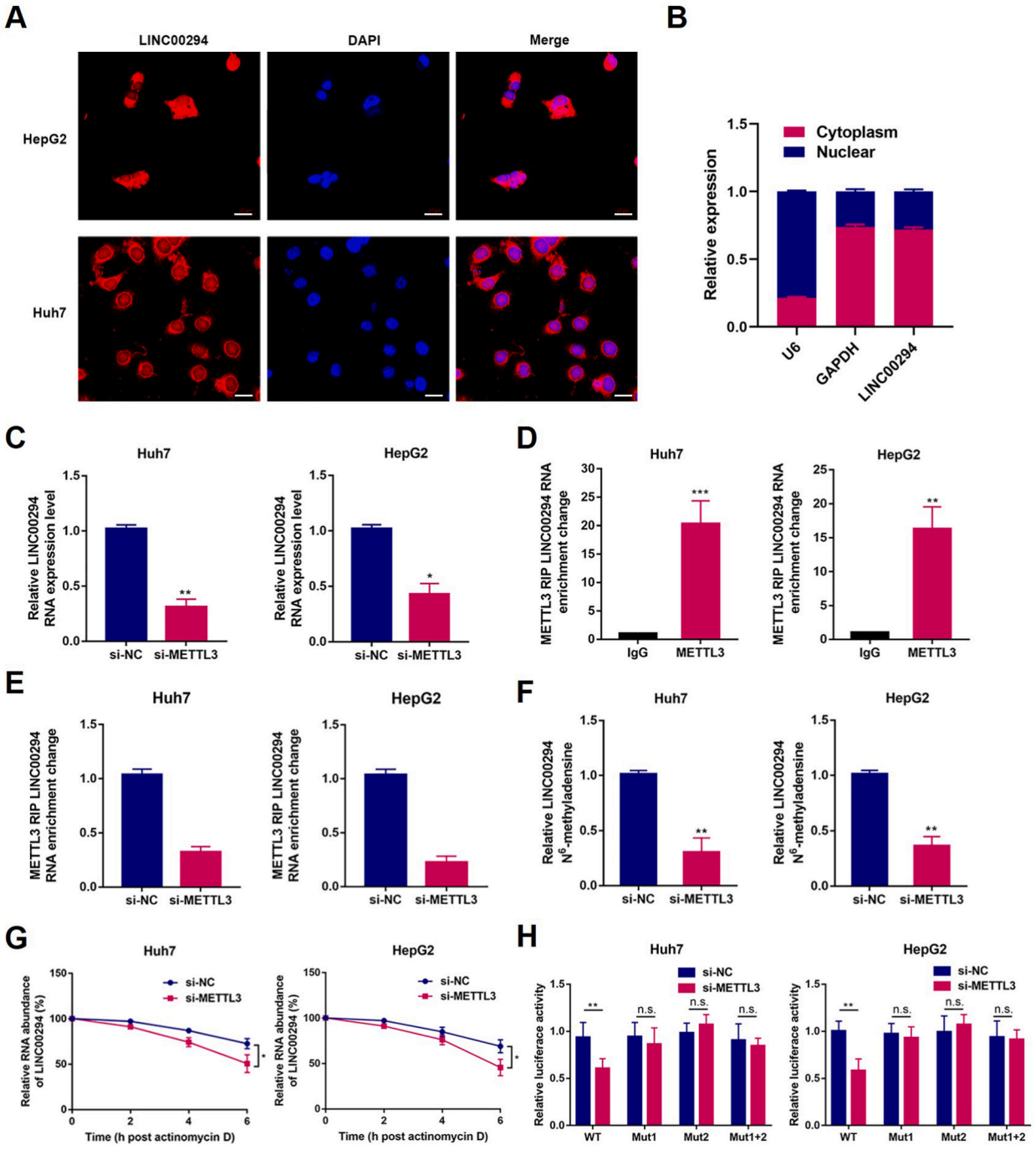

Fig. 4. METTL3 increases m^{6}A modification and expression of LINC00294. (A) FISH was performed to observe the cellular location of LINC00294 (scale bar, 20 μm). **(B)** The LINC00294 expression levels in the nucleus and cytoplasm was determined by qPCR. **(C)** RT-qPCR was used to detect LINC00294 expression levels in Huh7 and HepG2 cells with METTL3 knockdown. **(D)** RIP-qPCR was used to analyze the enrichment of METTL3 on LINC00294 in HCC cells compared with the IgG control. **(E)** RIP-qPCR assay was performed to identify the interaction between METTL3 and LINC00294 in HCC cells with knockdown of METTL3. **(F)** MeRIP-qPCR was used to test the relative levels of m^{6}A in LINC00294 in HCC cells with knockdown of METTL3. **(G)** The RNA lifetime of LINC00294 in HCC cells with or without METTL3 silencing. **(H)** Relative activity of the WT or Mut luciferase reporters in METTL3-silenced HCC cells was determined (normalized to negative control groups). *$p < 0.05$, **$p < 0.01$, ***$p < 0.001$; n. s, no significance.

3.3. LINC00294 drives glycolytic metabolism in HCC

The rates of lactate synthesis and glucose absorption were assessed using functional colorimetric assays. Knockdown of LINC00294 produced significant decreases in glucose uptake and lactate synthesis, whereas the overexpression of LINC00294 significantly increased lactic acid production as well as glucose consumption in HepG2 and Huh7 cells (Fig. 3A and B). To examine whether the expression of LINC00294 directly influences glycolytic metabolism, we tested the ECAR in HCC cells after manipulation of LINC00294 expression. Knockdown of LINC00294 significantly reduced ECAR levels compared with those of control cells, whereas LINC00294 overexpression markedly improved ECAR levels in HCC cells (Fig. 3C).

3.4. METTL3 increases the m^{6}A modification and expression of LINC00294

Given that the specific regulatory mechanism of lncRNA expression is associated with its cellular localization, an immunofluorescence assay was used to identify that LINC00294 was enriched both the nuclei and cytoplasm of the HCC cells (Fig. 4A). The LINC00294 expression levels in the nucleus and cytoplasm was determined by qPCR (Fig. 4B). To examine the regulatory role of m^{6}A modification in the expression of LINC00294, the m^{6}A target database (http://m6a2target.canceromics.org/#/) [24] was used to obtain information on LINC00294 m^{6}A modification. Predicted results indicated that LINC00294 may be modified by METTL3. RT-qPCR results showed that LINC00294 expression levels decreased with METTL3 knockdown in HepG2 and Huh7 cells (Fig. 4C). We found higher enrichment of METTL3 on LINC00294 compared with the IgG control using the RIP-qPCR assay (Fig. 4D). METTL3 silence also inhibited this interaction in HCC cells (Fig. 4E). Furthermore, the MeRIP-qPCR assay revealed that a decreased m^{6}A level of LINC00294 was observed with METTL3 knockdown (Fig. 4F). Moreover, METTL3 disruption exhibited lower mRNA stability after treatment with actinomycin D (Fig. 4G). m^{6}A sites of LINC00294 were predicted using the SRAMP database (http://www.cuilab.cn/

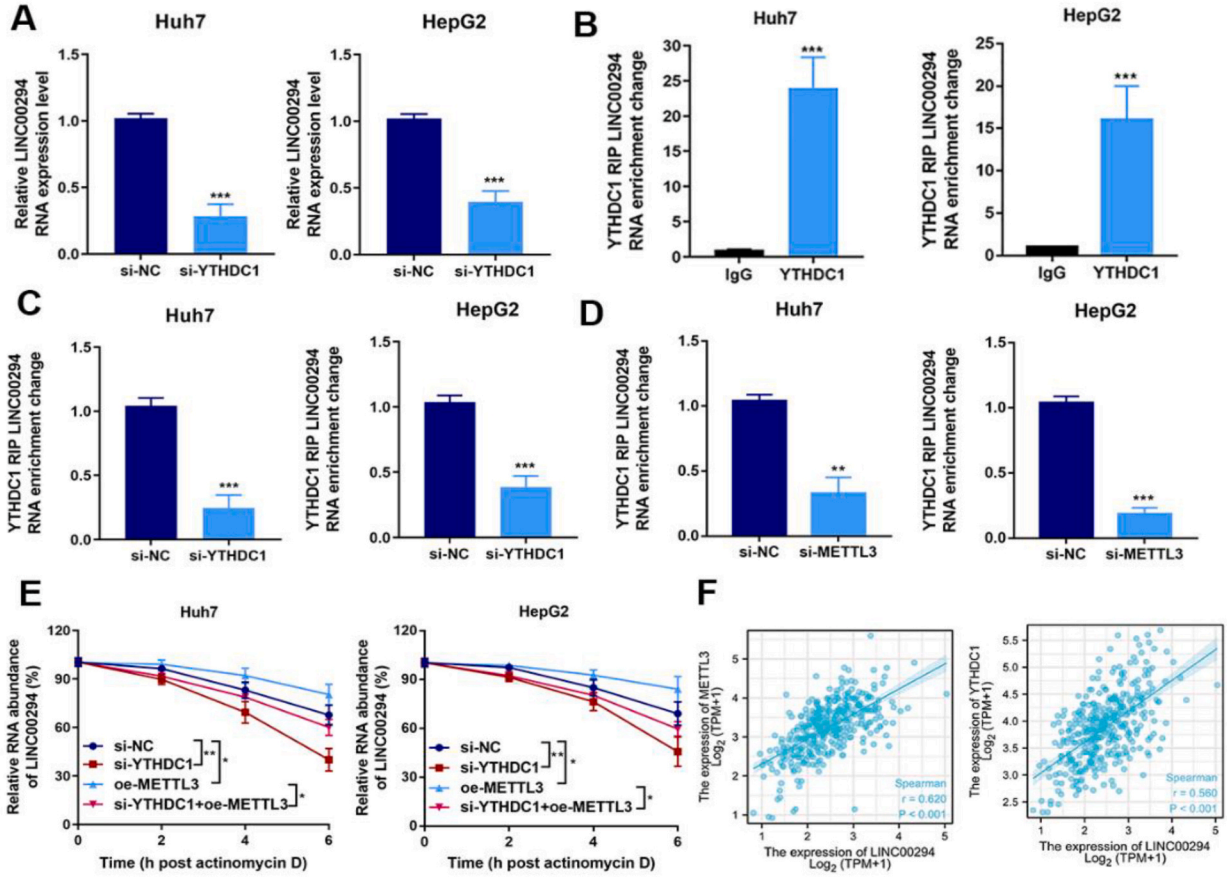

Fig. 5. YTHDC1 mediates LINC00294 expression in an m^{6}A-dependent manner. (A) RT-qPCR was used to detect LINC00294 expression levels in Huh7 and HepG2 cells with YTHDC1 knockdown. **(B)** RIP-qPCR was used to analyze the enrichment of YTHDC1 on LINC00294 in HCC cells compared with the IgG control. **(C)** RIP-qPCR assay was performed to identify the interaction between YTHDC1 and LINC00294 in HCC cells with knockdown of YTHDC1. **(D)** RIP-qPCR assay was used to detect the enrichment of YTHDC1 on LINC00294 in control and METTL3-knockdown cells. **(E)** RT-qPCR was used to determine the LINC00294 expression levels in HCC cells after actinomycin D treatment. **(F)** Correlation analysis showed the positive correlation between LINC00294 and METTL3 or YTHDC1 expression in TCGA data sets. *p < 0.05, **p < 0.01, ***p < 0.001.

sramp) [23], the relative luciferase activity of WT decreased upon METTL3 knockdown, but silencing METTL3 had no effect on Mut groups (Supplementary figure 2 and fig. 4H). Our results suggest that LINC00294 expression and stability are regulated by METTL3-mediated m^{6}A modification.

3.5. YTHDC1 mediates the LINC00294 expression in an m^{6}A-dependent manner

To investigate the fundamental process of METTL3-promoted LINC00294 expression, earlier studies inspired us to consider that METTL3 could recruit "m^{6}A readers" to enhance the stability of their target transcript. We found that knockdown of YTHDC1, a critical member of m^{6}A binding proteins, decreased the LINC00294 expression levels in HCC cells (Fig. 5A). To confirm whether YTHDC1 is a possible reader of LINC00294 m^{6}A methylation, the binding interaction between YTHDC1 and LINC00294 was measured via RIP-qPCR assay (Fig. 5B), and YTHDC1 knockdown successfully attenuated this binding relationship (Fig. 5C). The effects of YTHDC1 on LINC00294 binding were abrogated upon METTL3 knockdown (Fig. 5D), suggesting a regulatory role for METTL3. Additionally, YTHDC1 silencing reduced the mRNA stability of LINC00294, and knocking of YTHDC1 could reverse the increased LINC00294 stability mediated by METTL3 overexpression (Fig. 5E). Analysis of TCGA data also indicated that LINC00294 expression was positively correlated with METTL3 and YTHDC1 (Fig. 5F).

3.6. METTL3/YTHDC1 regulates LINC00294 expression in HCC cells

To examine the function of METTL3 or YTHDC1 in LINC00294-mediated tumor proliferation and aerobic glycolysis, CCK8 assay

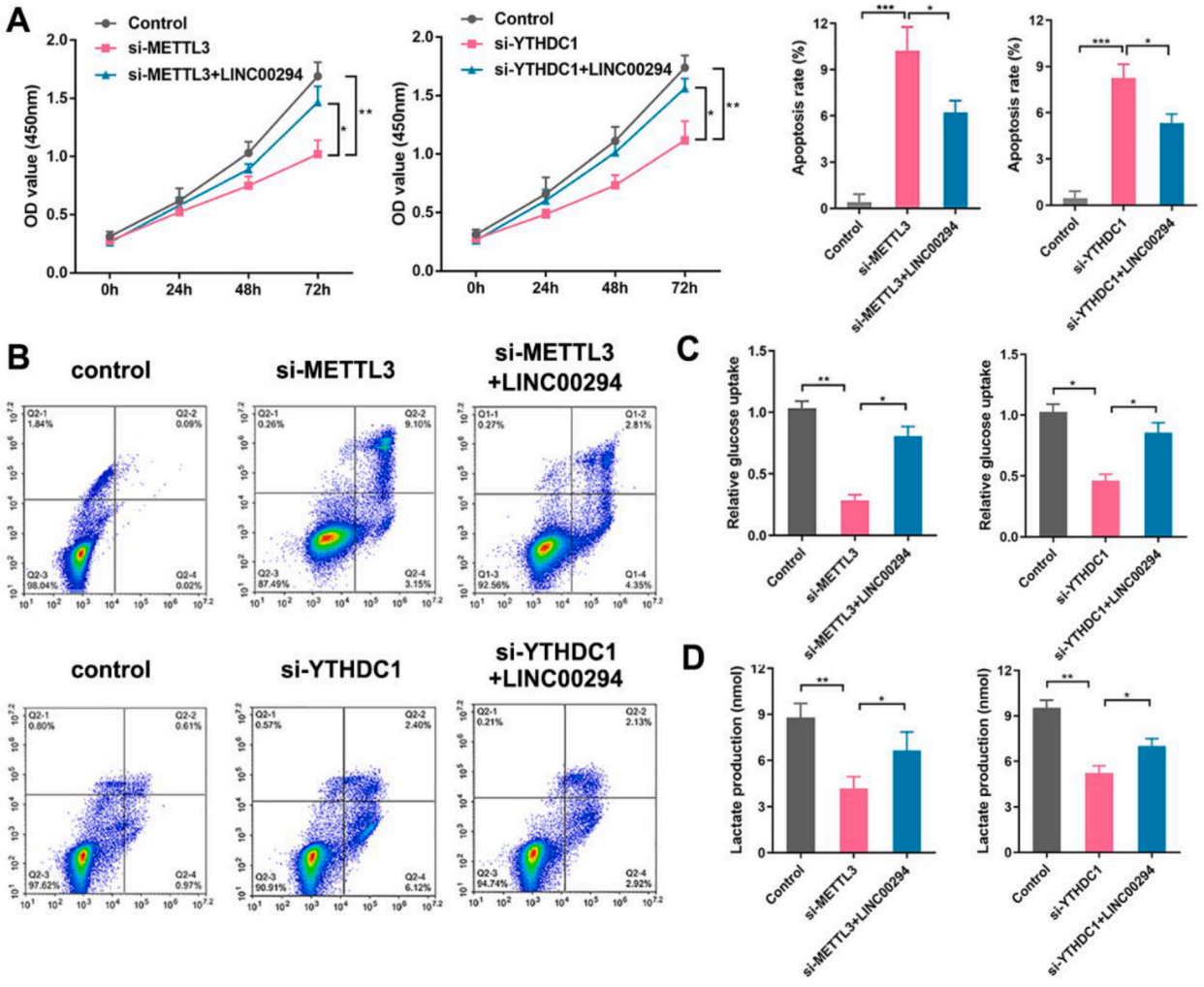

Fig. 6. METTL3/YTHDC1 functions by regulating LINC00294 Expression in HCC cells. (A) The CCK8 assay was performed in Huh7 cells with indicated transfection. **(B)** The apoptosis rate in Huh7 cells with indicated transfection. **(*C*–D)** Glucose uptake (C) and lactate production (D) were measured via colorimetric analysis. *p < 0.05, **p < 0.01, ***p < 0.001.

results revealed that METTL3-, YTHDC1-knockdown could decrease the proliferation in HepG2 cells in contrast with that in the control group and that these effects could be attenuated by the overexpression of LINC00294 (Fig. 6A). The apoptotic rates were improved with knockdown of METTL3 or YTHDC1, whereas the overexpression of LINC00294 could rescue these effects (Fig. 6B). In addition, the overexpression of LINC00294 significantly restored the decrease in glucose uptake when METTL3 or YTHDC1 was depleted (Fig. 6C). The overexpression of LINC00294 also reversed the decrease in lactate production in HepG2 METTL3/YTHDC1-silence cells in glycolytic assays (Fig. 6D).

3.7. *LINC00294 regulates HK2 and GLUT1 mRNA dependent on the presence of YTHDC1*

HK2 and GLUT1 are crucial enzymes in aerobic glycolysis, and we consequently performed the RIP-qPCR assay to detect the binding link between YTHDC1 and HK2 and GLUT1 mRNA. The results showed a higher enrichment of YTHDC1 with HK2 and GLUT1 mRNA relative to the IgG control, and the reduction of LINC00294 expression blunted this binding interaction (Fig. 7A). Moreover, western blotting and RT-qPCR results demonstrated that knockdown of YTHDC1 and LINC00294 decreased the protein and mRNA expression of HK2 and GLUT1, whereas LINC00294 overexpression could reverse the YTHDC1-induced effect (Fig. 7B and C). Silencing YTHDC1 expression also reduced the stability of HK2 and GLUT1 mRNA, and the overexpression of LINC00294 could reverse this effect (Fig. 7D). In addition, results of correlation analysis showed that the expression of GLUT1/SLC2A1 and HK2 were positive correlated with the expression of LINC00294, and YTHDC1, respectively (Fig. 7E).

4. Discussion

The advancement of high-throughput sequencing technologies has contributed to the identification of lncRNA expression as a marker for various diseases, such as developmental abnormalities, neuromuscular diseases, and tumors [4,9,11]. LINC00294, a newly described intergenic lncRNA, plays a role in the onset and progression of several tumors [16–18]. However, the function and regulatory role of LINC00294 in HCC remains unclear and requires further investigation. Herein, our results confirmed that LINC00294 expression was upregulated in HCC samples and exhibited a correlation with the unfavorable prognosis of patients with HCC. We also analyzed the diagnostic value of LINC00294 expression via ROC analysis. Additionally, knock down of LINC00294 attenuated the proliferation, apoptosis rate, and glycolysis of HCC cells in vitro, whereas the overexpression of LINC00294 exerted the opposite effects. Furthermore, LINC00294 mediated the growth of tumors in murine xenograft models.

Epigenetic regulation is crucial in controlling gene expression, and RNA methylation, a post-transcriptional modification, has gained widespread attention. m^6A modifications have been identified as the most prevalent internal modification and are involved in multiple physiological processes and disease pathogenesis, including RNA stability, structure switching, and protein translation [19,20]. lncRNAs, a sub-type of non-coding RNAs of >200 nucleotides in length, can be regulated by m^6A modification in various biological processes. lncRNA DANCR is reported to be instrumental in the onset and progression of a wide variety of cancers. IGF2BP2, which is an m^6A reader, contributes to the carcinogenicity of pancreatic cancer by modifying DANCR [25]. ALKBH5, a key

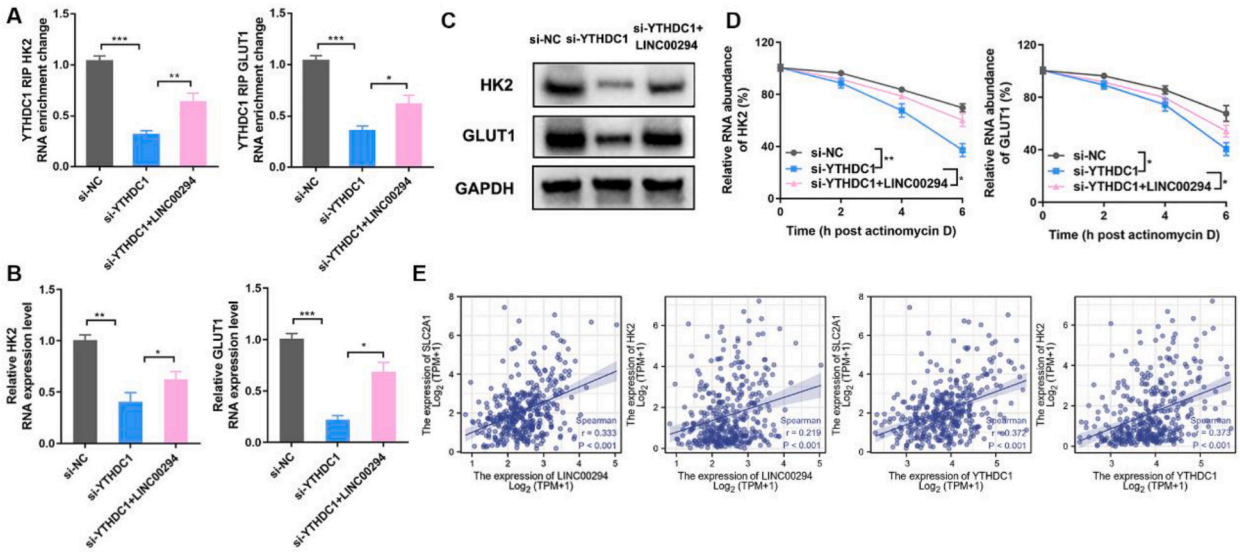

Fig. 7. LINC00294 promotes the association between YTHDC1 and HK2 and GLUT1 mRNA. (A) RIP-qPCR assay was performed to identify the interaction between YTHDC1 and HK2 or GLUT1 mRNA in Huh7 cells with indicated transfection. **(B–C)** RT-qPCR and Western blot were used to analyze the HK2 and GLUT1 mRNA and protein expression levels in the indicated groups. The uncropped Western blot images are in the Supplementary Fig. 3. **(D)** The mRNA lifetime of HK2 and GLUT1 in Huh7 cells with indicated transfection. **(E)** Correlation between the expression levels of the indicated molecules in the TCGA database of liver cancer. *p < 0.05, **p < 0.01, ***p < 0.001.

demethylase, which prompts the cell growth of glioblastoma stem-like cells (GSCs), is promoted by a lncRNA antisense to forkhead box M1 (FOXM1-AS) to interact with FOXM1 nascent transcripts to enhance the expression of FOXM1 and proliferation of GSCs [26]. YTHDF2 recognizes m^6A methylated sites of lnc-Dpf3 and strengthens the binding interaction between lnc-Dpf3 and HIF-1α, causing the inhibition of the migration as well as the aerobic glycolysis of dendritic cells [27]. In this study, we explored a new regulatory mechanism for LINC00294 in HCC. Given the significance of cellular localization in LINC00294 functions, we discovered that LINC00294 was present in both the nuclei and cytoplasm of HCC cells, suggesting that the LINC00294 may be modulated by the nucleus-located process and is implicated in post-transcriptional modulation via interactions with RNA-binding proteins. Furthermore, using bioinformatic prediction, LINC00294 was shown to act as a prospective downstream target of METTL3-mediated m^6A alteration in HCC cells. Our results support the hypothesis that METTL3 directly interacts with LINC00294 to regulate m^6A modification of LINC00294. The m^6A reader YTHDC1 is recruited by METTL3 and could bind to LINC00294 in a METTL3/m^6A-dependent manner to synergistically enhance the stability of LINC00294. Furthermore, we observed a significant positive correlation in TCGA data sets between the expression of LINC00294 and METTL3 or YTHDC1.

Our data demonstrated that METTL3 and YTHDC1 could both accelerate HCC cell proliferation and reduce the apoptosis and glycolysis process through regulating LINC00294 expression. These results illustrated that YTHDC1 and METTL3 may have an oncogenic role in the onset and progression of HCC. METTL3 has been shown to regulate m^6A modification of HDGF and recruit IGF2BP3 as the m^6A reader to bind the m^6A site and promote RNA stability of HDGF, leading to the interaction between nuclear HDGF and GLUT4 and ENO2 in HCC cells [28]. HBXIP-mediated METTL3 has been shown to increase the m^6A modification of HIF-1α, promoting the metabolic reprogramming and malignant biological behaviors of HCC cells [29]. METTL3 expression is also positively correlated with glycolysis metabolism in HCC. YTHDC1 is an m^6A reader that nearly completely shares domains with m^6A modification in nuclear RNA molecules. miR-30d, which is a specific target for YTHDC1-mediated m^6A modification can reportedly inhibit pancreatic tumorigenesis via suppressing the RUNX1-SLC2A1/HK1 axis to block glycolysis [30]. The m^6A-modified hsa_circ_0058493 can also bind to YTHDC1 to mediate the progression of HCC, thus promoting the intracellular localization of hsa_circ_0058493 from the nucleus to the cytoplasm [31]. Interestingly, our findings agreed with these results, demonstrating the integral function of YTHDC1 and METTL3 in HCC tumorigenesis and the cancerous Warburg effect.

This study revealed a novel regulatory mechanism of HK2 and GLUT1 expression in HCC. HK2 [32–34] and GLUT1 [35–38] are the crucial hub enzymes for aerobic glycolysis or the Warburg effect. Our results indicated a significantly higher enrichment of YTHDC1 with HK2 and GLUT1 mRNA, whereas these interactions were reversed by LINC00294 inhibition. Furthermore, YTHDC1 silencing decreased the RNA stability and expression levels of HK2 and GLUT1 mRNA, whereas the overexpression of LINC00294 reversed this effect, suggesting that LINC00294 also plays an integral role in YTHDC1-HK2/GLUT1 axis regulation. Recent research into the processes of lncRNA has illustrated the complex interactions between lncRNAs, RNA binding proteins, and the RNAs that they target [39]. Consequently, continued investigation into how the regulatory role of LINC00294 affects YTHDC1 in the context of interacting with HK2 and GLUT1 is warranted.

Overall, our study suggested that LINC00294 plays a significant carcinogenic role and may serve as a biological marker for HCC. Our study proposed a new mechanism for METTL3/YTHDC1-regulated m^6A modification of LINC00294 and, as a feedback regulation, LINC00294 was involved in the interaction between YTHDC1 and HK2 or GLUT1 mRNA in HCC cells (Fig. 8). Therefore, from the diagnosis and treatment perspective, this study demonstrates that the expression of LINC00294 in HCC was related to the progression of HCC. Thus, LINC00294 may be regarded as a judgment marker of malignant degree and prognosis of HCC, and more research is required to validate this. Furthermore, the mechanism of LINC00294-induced tumor growth and glucose metabolism in cellular regulation will enable the identification of new targets.

Funding

This work was sponsored in part by the National Natural Science Foundation of China (No. 82072892), the Natural Science Foundation of Shanghai (No. 21ZR1454900), the Guangxi Natural Science Foundation (No.2023GXNSFAA026276) and Key Medical Discipline Project of Shanghai Jiading District (No. 2020-jdyxzdxk-13).

Data availability statement

Data included in article/supp. material/referenced in article.

Ethics approval and consent to participate

This study was carried out in accordance with the recommendations of The Shanghai General Hospital Clinical Center Laboratory Animal Welfare & Ethics Committee (2022AW026) and the Ethics Committees of Shanghai General Hospital (SHYJS-CP-1701102).

Consent for publication

Not applicable.

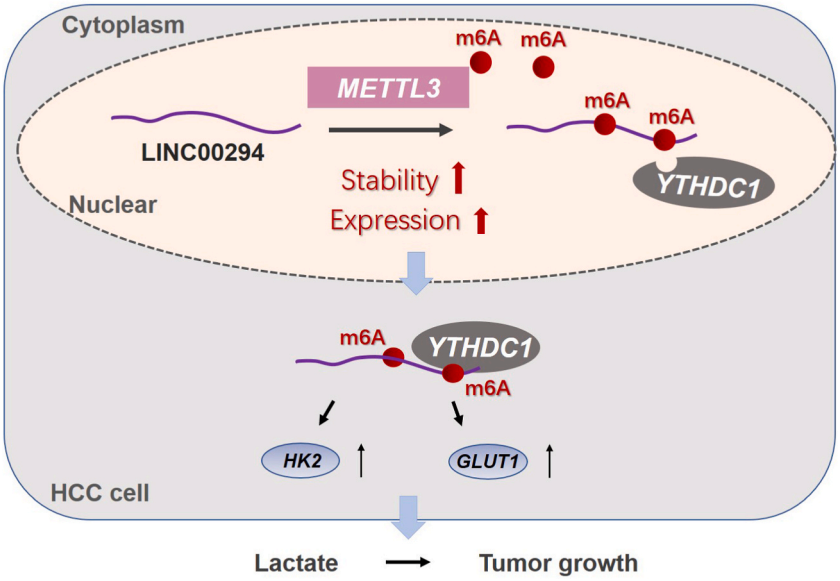

Fig. 8. Model for how LINC00294 was involved in the interaction between YTHDC1 and HK2 or GLUT1 mRNA in HCC cells.

CRediT authorship contribution statement

Rulin Zhang: Writing – original draft, Methodology, Investigation, Data curation. **Rui Yang:** Project administration, Investigation, Data curation. **Zhuodeng Huang:** Formal analysis, Data curation. **Xiang Xu:** Formal analysis, Data curation. **Siang Lv:** Writing – review & editing, Validation. **Xin Guan:** Writing – review & editing, Validation. **Hao Li:** Supervision, Project administration, Investigation. **Jun Wu:** Writing – review & editing, Writing – original draft, Supervision, Project administration, Investigation, Funding acquisition, Formal analysis, Conceptualization.

Declaration of competing interest

The authors declare that they have no known competing financial interests or personal relationships that could have appeared to influence the work reported in this paper.

Acknowledgements

Not applicable.

Appendix A. Supplementary data

Supplementary data to this article can be found online at https://doi.org/10.1016/j.heliyon.2023.e22595.

References

[1] R.L. Siegel, K.D. Miller, H.E. FuchsA. Jemal, Cancer statistics, CA Cancer J Clin 72 (1) (2022) 7–33, 2022.
[2] A. Villanueva, Hepatocellular carcinoma, N. Engl. J. Med. 380 (15) (2019) 1450–1462.
[3] L. Miao, Z. Zhang, Z. RenY. Li, Application of immunotherapy in hepatocellular carcinoma, Front. Oncol. 11 (2021), 699060.
[4] M. Homayoonfal, Z. AsemiB. Yousefi, Targeting long non coding RNA by natural products: implications for cancer therapy, Crit. Rev. Food Sci. Nutr. 63 (20) (2023) 4389–4417.
[5] A. Sanchez Calle, Y. Kawamura, Y. Yamamoto, F. TakeshitaT. Ochiya, Emerging roles of long non-coding RNA in cancer, Cancer Sci. 109 (7) (2018) 2093–2100.
[6] B. Giuliani, C. TordonatoF. Nicassio, Mechanisms of long non-coding RNA in breast cancer, Int. J. Mol. Sci. 24 (5) (2023).
[7] S. Nandagopal, S. Misra, S. Sankanagoudar, M. Banerjee, P. Sharma, S.E. Pane, G. GuerrieroK, K. Shukla, Long non coding RNA in triple negative breast cancer: a promising biomarker in tumorigenesis, Asian Pac J Cancer Prev 24 (1) (2023) 49–59.
[8] E. Bozgeyik, Variations in genomic regions encoding long non-coding RNA genes associated with increased prostate cancer risk, Mutat. Res. Rev. Mutat. Res. 791 (2023), 108456.
[9] M. Hashemi, M.S. Moosavi, H.M. Abed, M. Dehghani, M. Aalipour, E.A. Heydari, M. Behroozaghdam, M. Entezari, S. Salimimoghadam, E.S. Gunduz, A. Taheriazam, S. MirzaeiS. Samarghandian, Long non-coding RNA (lncRNA) H19 in human cancer: from proliferation and metastasis to therapy, Pharmacol. Res. 184 (2022), 106418.
[10] L. Luo, M. Wang, X. Li, J. Tian, K. Zhang, S. TanC. Luo, Long non-coding RNA LOC285194 in cancer, Clin. Chim. Acta 502 (2020) 1–8.

[11] U. Sharma, T.S. Barwal, A. Malhotra, N. Pant, Vivek, D. Dey, A. Gautam, H.S. Tuli, K.M. VasquezA. Jain, Long non-coding RNA TINCR as potential biomarker and therapeutic target for cancer, Life Sci. 257 (2020), 118035.
[12] X. Gu, Q. Zheng, Q. ChuH. Zhu, HAND2-AS1: a functional cancer-related long non-coding RNA, Biomed. Pharmacother. 137 (2021), 111317.
[13] L. Barros Ferreira, L.M. Ashander, B. Appukuttan, Y. Ma, K.A. WilliamsJ, R. Smith, Expression of long non-coding RNAs in activated human retinal vascular endothelial cells, Ocul. Immunol. Inflamm. (2022) 1–6.
[14] X. Zhang, T. Han, T. Xu, H. WangH. Ma, Uncovering candidate mRNAs, signaling pathways and immune cells in atherosclerotic plaque and ischemic stroke, Int. J. Gen. Med. 16 (2023) 2999–3012.
[15] J. Xu, H. Feng, L. Ma, H. Tan, S. YanC. Fang, Bakkenolide-IIIa ameliorates lipopolysaccharide-induced inflammatory injury in human umbilical vein endothelial cells by upregulating LINC00294, Mol. Med. Rep. 23 (5) (2021).
[16] J. Qiu, S. Zhou, W. ChengC. Luo, LINC00294 induced by GRP78 promotes cervical cancer development by promoting cell cycle transition, Oncol. Lett. 20 (5) (2020) 262.
[17] X. Zhou, L. Lv, Z. Zhang, S. WeiT. Zheng, LINC00294 negatively modulates cell proliferation in glioma through a neurofilament medium-mediated pathway via interacting with miR-1278, J. Gene Med. 22 (10) (2020) e3235.
[18] P. Qi, Z. Yexie, C. Xue, G. Huang, Z. ZhaoX. Zhang, LINC00294/miR-620/MKRN2 axis provides biomarkers and negatively regulates malignant progression in colorectal carcinoma, Hum. Exp. Toxicol. 42 (2023), 9603271231167577.
[19] J. Liu, B.T. HaradaC. He, Regulation of gene expression by N(6)-methyladenosine in cancer, Trends Cell Biol. 29 (6) (2019) 487–499.
[20] Y. Wang, Y. Wang, H. Patel, J. Chen, J. Wang, Z.S. ChenH. Wang, Epigenetic modification of m(6)A regulator proteins in cancer, Mol. Cancer 22 (1) (2023) 102.
[21] X. Cai, X. Wang, C. Cao, Y. Gao, S. Zhang, Z. Yang, Y. Liu, X. Zhang, W. ZhangL. Ye, HBXIP-elevated methyltransferase METTL3 promotes the progression of breast cancer via inhibiting tumor suppressor let-7g, Cancer Lett. 415 (2018) 11–19.
[22] H. Yin, X. Zhang, P. Yang, X. Zhang, Y. Peng, D. Li, Y. Yu, Y. Wu, Y. Wang, J. Zhang, X. Ding, X. Wang, A. YangR. Zhang, RNA m6A methylation orchestrates cancer growth and metastasis via macrophage reprogramming, Nat. Commun. 12 (1) (2021) 1394.
[23] T. Sun, C.C. Ding, Y. Zhang, Y. Zhang, C.C. Lin, J. Wu, Y. Setayeshpour, S. Coggins, C. Shepard, E. Macias, B. Kim, P. Zhou, R. GordànJ, T. Chi, MESH1 knockdown triggers proliferation arrest through TAZ repression, Cell Death Dis. 13 (3) (2022) 221.
[24] S. Deng, H. Zhang, K. Zhu, X. Li, Y. Ye, R. Li, X. Liu, D. Lin, Z. ZuoJ. Zheng, M6A2Target: a comprehensive database for targets of m6A writers, erasers and readers, Brief Bioinform 22 (3) (2021).
[25] X. Hu, W.X. Peng, H. Zhou, J. Jiang, X. Zhou, D. Huang, Y.Y. MoL. Yang, IGF2BP2 regulates DANCR by serving as an N6-methyladenosine reader, Cell Death Differ. 27 (6) (2020) 1782–1794.
[26] S. Zhang, B.S. Zhao, A. Zhou, K. Lin, S. Zheng, Z. Lu, Y. Chen, E.P. Sulman, K. Xie, O. Bögler, S. Majumder, C. HeS. Huang, m(6)A demethylase ALKBH5 maintains tumorigenicity of glioblastoma stem-like cells by sustaining FOXM1 expression and cell proliferation program, Cancer Cell 31 (4) (2017) 591–606.e6.
[27] J. Liu, X. Zhang, K. Chen, Y. Cheng, S. Liu, M. Xia, Y. Chen, H. Zhu, Z. LiX. Cao, CCR7 chemokine receptor-inducible lnc-dpf3 restrains dendritic cell migration by inhibiting HIF-1α-Mediated glycolysis, Immunity 50 (3) (2019) 600–615.e15.
[28] Q. Wang, C. Chen, Q. Ding, Y. Zhao, Z. Wang, J. Chen, Z. Jiang, Y. Zhang, G. Xu, J. Zhang, J. Zhou, B. Sun, X. ZouS. Wang, METTL3-mediated m(6)A modification of HDGF mRNA promotes gastric cancer progression and has prognostic significance, Gut 69 (7) (2020) 1193–1205.
[29] N. Yang, T. Wang, Q. Li, F. Han, Z. Wang, R. ZhuJ. Zhou, HBXIP drives metabolic reprogramming in hepatocellular carcinoma cells via METTL3-mediated m6A modification of HIF-1α, J. Cell. Physiol. 236 (5) (2021) 3863–3880.
[30] Y. Hou, Q. Zhang, W. Pang, L. Hou, Y. Liang, X. Han, X. Luo, P. Wang, X. Zhang, L. LiX. Meng, YTHDC1-mediated augmentation of miR-30d in repressing pancreatic tumorigenesis via attenuation of RUNX1-induced transcriptional activation of Warburg effect, Cell Death Differ. 28 (11) (2021) 3105–3124.
[31] A. Wu, Y. Hu, Y. Xu, J. Xu, X. Wang, A. Cai, R. Liu, L. ChenF. Wang, Methyltransferase-like 3-mediated m6A methylation of Hsa_circ_0058493 accelerates hepatocellular carcinoma progression by binding to YTH domain-containing protein 1, Front. Cell Dev. Biol. 9 (2021), 762588.
[32] C. Shen, B. Xuan, T. Yan, Y. Ma, P. Xu, X. Tian, X. Zhang, Y. Cao, D. Ma, X. Zhu, Y. Zhang, J.Y. Fang, H. ChenJ, Hong, m(6)A-dependent glycolysis enhances colorectal cancer progression, Mol. Cancer 19 (1) (2020) 72.
[33] Y. Fang, Z.Y. Shen, Y.Z. Zhan, X.C. Feng, K.L. Chen, Y.S. Li, H.J. Deng, S.M. Pan, D.H. WuY. Ding, CD36 inhibits β-catenin/c-myc-mediated glycolysis through ubiquitination of GPC4 to repress colorectal tumorigenesis, Nat. Commun. 10 (1) (2019) 3981.
[34] H.J. Lee, C.F. Li, D. Ruan, J. He, E.D. Montal, S. Lorenz, G.D. GirnunC, H. Chan, Non-proteolytic ubiquitination of Hexokinase 2 by HectH9 controls tumor metabolism and cancer stem cell expansion, Nat. Commun. 10 (1) (2019) 2625.
[35] X. Li, C. Jiang, Q. Wang, S. Yang, Y. Cao, J.N. Hao, D. Niu, Y. Chen, B. Han, X. Jia, P. ZhangY. Li, A "Valve-Closing" starvation strategy for amplification of tumor-specific chemotherapy, Adv. Sci. 9 (8) (2022), e2104671.
[36] Z. Zhang, X. Li, F. Yang, C. Chen, P. Liu, Y. Ren, P. Sun, Z. Wang, Y. You, Y.X. ZengX. Li, DHHC9-mediated GLUT1 S-palmitoylation promotes glioblastoma glycolysis and tumorigenesis, Nat. Commun. 12 (1) (2021) 5872.
[37] Y. Mo, Y. Wang, S. Zhang, F. Xiong, Q. Yan, X. Jiang, X. Deng, Y. Wang, C. Fan, L. Tang, S. Zhang, Z. Gong, F. Wang, Q. Liao, C. Guo, Y. Li, X. Li, G. Li, Z. ZengW. Xiong, Circular RNA circRNF13 inhibits proliferation and metastasis of nasopharyngeal carcinoma via SUMO2, Mol. Cancer 20 (1) (2021) 112.
[38] S. Ju, F. Wang, Y. WangS. Ju, CSN8 is a key regulator in hypoxia-induced epithelial-mesenchymal transition and dormancy of colorectal cancer cells, Mol. Cancer 19 (1) (2020) 168.
[39] A.R. Gawronski, M. Uhl, Y. Zhang, Y.Y. Lin, Y.S. Niknafs, V.R. Ramnarine, R. Malik, F. Feng, A.M. Chinnaiyan, C.C. Collins, S.C. SahinalpR. Backofen, MechRNA: prediction of lncRNA mechanisms from RNA-RNA and RNA-protein interactions, Bioinformatics 34 (18) (2018) 3101–3110.